

Journal of Materials Chemistry A

Accepted Manuscript



This is an *Accepted Manuscript*, which has been through the Royal Society of Chemistry peer review process and has been accepted for publication.

Accepted Manuscripts are published online shortly after acceptance, before technical editing, formatting and proof reading. Using this free service, authors can make their results available to the community, in citable form, before we publish the edited article. We will replace this *Accepted Manuscript* with the edited and formatted *Advance Article* as soon as it is available.

You can find more information about *Accepted Manuscripts* in the [Information for Authors](#).

Please note that technical editing may introduce minor changes to the text and/or graphics, which may alter content. The journal's standard [Terms & Conditions](#) and the [Ethical guidelines](#) still apply. In no event shall the Royal Society of Chemistry be held responsible for any errors or omissions in this *Accepted Manuscript* or any consequences arising from the use of any information it contains.

COMMUNICATION

Facile Synthesis of Titanium Nitride Nanowires on Carbon Fabric for Flexible and High-Rate Lithium Ion Batteries

Cite this: DOI: 10.1039/x0xx00000x

Muhammad-Sadeeq Balogun,^a Minghao Yu,^a Cheng Li,^a Teng Zhai,^a Yi Liu,^{a, b} Xihong Lu,^{a*} and Yexiang Tong^{a*}

Received 00th January 2012,

Accepted 00th January 2012

DOI: 10.1039/x0xx00000x

www.rsc.org/

Herein, we demonstrate the good performance of TiN nanowires as anode for lithium-ion batteries. The TiN nanowires exhibit high cyclic performance with 80% capacity retention after 100 cycles at 335 mA/g. Additionally, flexible full battery was fabricated with attractive flexibility and electrochemical performance.

Flexible devices have captivated tremendous interest in the exploration of lightweight flexible storage devices due to rapid development of portable electronic devices.¹⁻⁷ These flexible storage devices demand high energy and power densities which have given lithium-ion batteries (LIBs) an attentive opportunity for utilization since LIBs are agreeable power sources with high energy and power densities.⁸⁻¹¹ Base on this background, flexible LIBs becomes the state-of-art in the field of flexible, bendable and stretchable energy storage devices. Recently, many attentions have been focusing on the assembling of flexible LIBs and significant outcome have been reported. For instance, ZnCo₂O₄ nanowires/carbon cloth anodes for flexible LIBs have been reported by Liu et al.,¹² likewise, Yu et al. demonstrates three-dimensional hierarchical MoS₂ nanoflake array/carbon cloth as flexible LIBs anodes,¹³ flexible MoS₂-graphene hybrid paper for thin film LIBs,¹⁴ carbon nanotube/silicon composite fiber anode for flexible wire-shaped LIBs were also reported.¹⁵ However, it is still a fundamental objection to further fabricate flexible LIBs with remarkable electrochemical performance.

With respect to improving the high consumption of energy by humans, electrode materials applied in energy storage devices becomes vigorously important.¹⁶⁻²⁰ Titanium Nitride (TiN), which is a well-known material for several applications,²¹⁻²³ has been considered as an attractive candidate as electrode material in energy storage devices²⁴⁻²⁷ due to its good electrical conductivity (4000–55500 S/cm),^{28,29} high chemical and thermal stability.³⁰ In LIBs electrode materials, TiN was often used as a coating material in order to improve the conductivity of the coated materials. For instance, they combined with other electrode materials forming nanocomposites³¹ such as Li₄Ti₅O₁₂/TiN,³² Si/TiN,³³ SnO₂/TiN³⁴ and hence, the nanocomposites exhibits high electrochemical performance.³⁵ Less attention has been given to utilizing TiN as

LIBs electrode active materials. Recently, Cui and his co-workers have demonstrated titanium vanadium nitride and carbon nanocomposites in their work reporting an attractive electrochemical performance of about 650 mAh/g at 74.4 mA/g and 200 mAh/g for the TiN/C composites.³⁶ Also, Lei et al. also demonstrates TiN/C nanocomposites reporting a discharge capacity of 76 mAh/g at 50 mA/g after 200 cycles.³⁷ The discharge capacities delivered by Cui's and Lei's group were still not high enough and still needs further improvement. Thus, it is still a vital challenge to synthesized TiN with high discharge capacities.

Recently, we have studied the instability mechanism of TiN nanowire supercapacitor electrodes and the irreversible electrochemical oxidation and structural breakdown are responsible for their capacitance loss.³⁰ We found that the stabilized TiN nanowires with a poly(vinyl alcohol) (PVA)/KOH gel exhibited excellent capacitive properties when as supercapacitor electrodes. In this communication, we extend the application of the TiN nanowires as high-rate anode for LIBs, and demonstrated a flexible high-performance full LIB device based on a TiN nanowire anode and a LiCoO₂ cathode for the first time. The as-prepared TiN nanowires exhibited an excellent rate performance, achieving a high capacity of 288 mAh/g at a high current density of 1675 mA/g. Additionally, it also has outstanding cyclic stability, which delivered a reversible capacity of 567 mAh/g at 1st cycle and could retain 455 mAh/g after 100 cycles at current density of 335 mA/g. Moreover, the TiN NW was used as anode in the demonstration of a flexible LIB device employing LiCoO₂ as the cathode. This fabricated LiCoO₂/TiN flexible lithium-ion battery device delivers an outstanding flexibility and good cyclic performance which could develop of more flexible LIBs.

TiN nanowires were synthesized on a carbon cloth by two-step approach (see Methods in the Supporting Information, SI). TiO₂ nanowires were first grown on the carbon cloth via hydrothermal method reported elsewhere.³⁸ The surface of the carbon cloth fibers was covered by single-crystalline TiO₂ nanowires with a diameters in a typical range between of 100 and 200 nm and lengths of about 1.5 μm (Figure S1). The TiO₂ nanowires were then annealed in ammonia (NH₃) gas at 800, 900 and 1000 °C to transform them to TiN nanowires (denoted as TiN-800, TiN-900 and TiN-1000 respectively). Scanning electron microscopy (SEM) analyses affirm that that the morphology of the annealed TiO₂ remains unchanged

after thermal treatment at 800, 900 and 1000 °C (Figure 1a-b and Figure S2). Figure 1c display a typical transmission electron microscopy (TEM) image of TiN-900 sample, showing the TiN nanowire has a diameter of about 160 nm. The selected area electron diffraction (SAED) pattern confirmed that the TiN nanowire is a single crystal with cubic structure (Figure 1c inset). The high-resolution TEM (HRTEM) image collected at the nanowire edge disclosed that the nanowires of the TiN has lattice fringes of 0.295 nm, which was designated to “110” of the cubic TiN phase (Figure 1d).

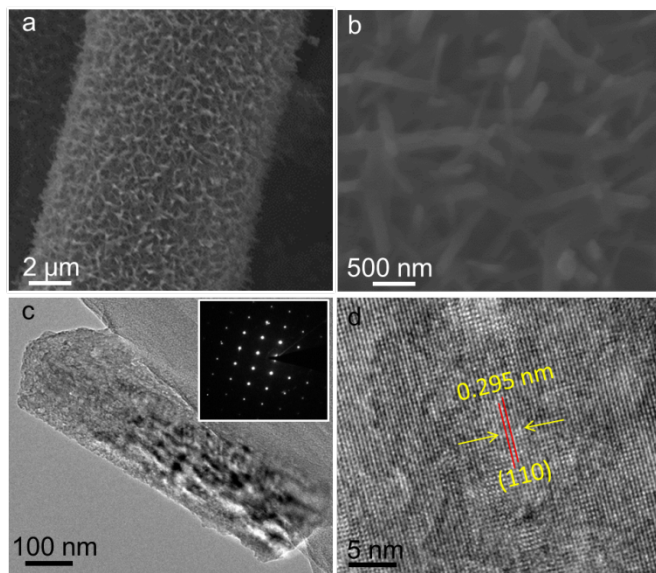


Figure 1. (a, b) SEM images, (c) TEM image and (d) HRTEM image of the TiN-900 sample. Inset in Figure 1c is the corresponding SAED pattern.

To understand more about the transformation of TiO₂ to TiN nanowires, further characterizations were carried out. X-ray diffraction spectra (XRD) reveal the transformation of rutile TiO₂ to cubic TiN when the TiO₂ nanowires are annealed in NH₃ at 800, 900 and 1000 °C (Figure 2a).³⁹⁻⁴¹ It can also be observed that the intensity of the TiN nanowires increases with increasing temperature also indicating successful transformation of TiO₂ into TiN and high crystallinity of the TiN. Raman spectra collected to determine the composition of the TiO₂ nanowires and after annealing in NH₃ gas shows characteristic peaks of TiN nanowires at 208, 313 and 552 cm⁻¹ in Figure 2b. Each TiN peaks shifted slightly towards the lower wavelength of the TiO₂. This can be attributed to the formation of Ti³⁺ during nitridation.^{30, 42} The peaks at 1333 and 1607 cm⁻¹ corresponds to the D and G bands from the carbon fabric. Investigations on the surface chemical composition changes and oxidation states of TiO₂ and after transformation to TiN nanowires were determined by X-ray photoelectron spectroscopy (XPS). XPS survey spectra collected from TiO₂ and TiN samples confirm the presence of nitrogen at a binding energy of about 400 eV in the TiN nanowires without any traces of nitrogen in the TiO₂ nanowires (Figure S3a). It was observed in the spectra collected from the N 1s core level that the characteristic peaks at binding energies of 396.5, 397.5 and 399.2 eV corresponds to Ti-N, Ti-N-O and adsorbed N₂ peaks respectively (Figure 2c).^{43, 44} Multiple peaks are evolved at lower binding energies in the Ti 2p spectra for the TiN nanowires samples resulting from the deconvolution of TiO₂ Ti 2p binding energy at 459.3 eV, which can be assigned as Ti 2p_{3/2}. The peaks at 455.8 eV, 457.1 eV and 458.7 eV can be associated with Ti-N,

Ti-N-O and Ti-O peaks respectively (Figure 2d).⁴³ Details about the O 1s core level were discussed Figure S3a. These outcomes justifies that the chemical states on surfaces of the TiN nanowires samples comprises of Ti-N-O, Ti-N, and Ti-O. The result obtained from the XRD, Raman and XPS also confirmed the transformation of TiO₂ nanowires into TiN nanowires.

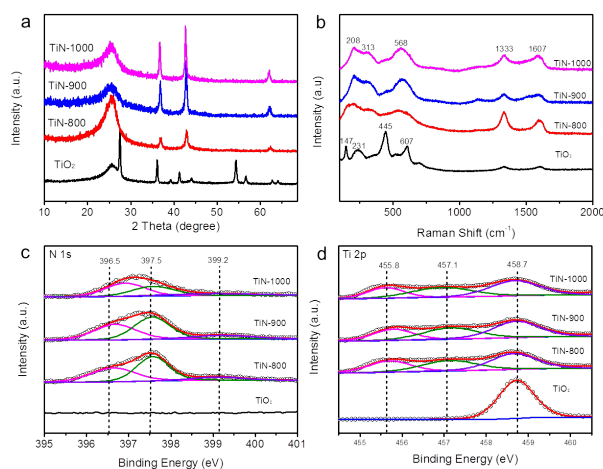
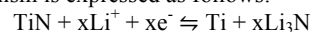


Figure 2. (a) XRD spectra, (b) Raman spectra, (c) core level N 1s XPS spectra and (d) core level Ti 2p XPS spectra of the TiO₂, TiN-800, TiN-900 and TiN-1000 samples.

Electrochemical performance was investigated to figure out the influence of lithium insertion and extraction process in the TiN electrodes. We first study the lithium storage mechanism in the TiN electrodes using the cyclic voltammograms (CV). The CV curves of the 1st cycle of the samples at a scan rate of 0.1 mVs⁻¹ over a voltage range of 0.01 - 3.0 V (vs Li⁺/Li) were shown in Figure S4a. During the first discharge cycle, three redox peaks were observed at 1.53/1.80 V, 0.74/0.92 V and 0.57/0.45 V. The peaks at the high voltage region (1.53/1.80 V) can be seen clearly Figure S4b. The reduction peaks corresponds to the reduction of TiN to Ti and oxidation peaks corresponds to the oxidation of Ti back to TiN. This indicates that high reversible insertion and extraction of Li⁺ in the TiN electrodes as indicated in the redox reaction.^{45, 46} The possible reaction mechanism is expressed as follows:



Very intense redox peaks were observed at low voltage region. This can be associated with the redox behavior of the carbon fabric.⁴⁵ The redox peaks noticed in the CV curves were persistent with the charge-discharge curves of the TiN electrodes (Figure 3b). The charge/discharge curves of the TiN electrodes after the first cycle shows that TiN-900 exhibits highest reversibility of 567 mAh/g which is higher than that of TiN-800 at 496 mAh/g and TiN-1000 at 478 mAh/g (Figure 3b). A coulombic efficiency of 86% was calculated for the TiN-900 after the second cycle which later increases to 97% in the third cycle and approximately 100% at the 100th cycle (Figure S5). The capacity loss after the first cycle is most likely due to the irreversible reactions by the formation of the solid electrolyte interface (SEI) layer^{31, 47, 48} which can be seen from the shape difference between the discharge voltage profiles of the first and other continuous cycles up to 100 cycles (Figure S5).

Cycling stability is one of the most important characteristics for evaluating the life span of electrode materials. We demonstrated the cyclic stability of the TiN samples by carrying out a discharge-charge measurements at a current density of 335 mA/g. A

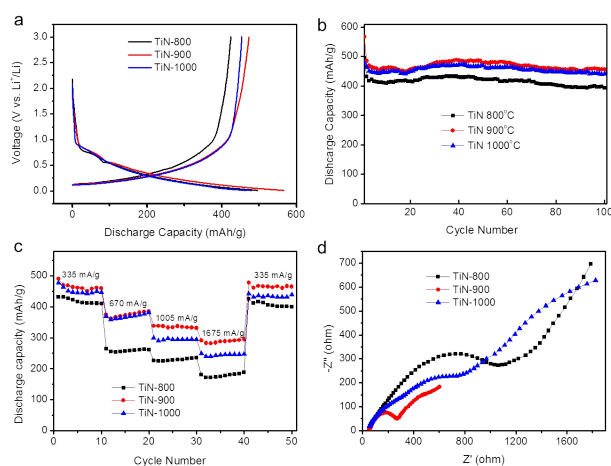


Figure 3. Electrochemical properties of the TiN electrodes. (a) Charge/discharge curves of the TiN electrodes. (b) Cycle performance of TiN electrodes at a voltage range of 0.01 – 3 V (vs. Li^+/Li) for 100 cycles. (c) Rate capability measurements of TiN electrodes at different current densities. (d) Nyquist plots of the TiN electrodes at a frequency range of 100 kHz to 0.01 Hz.

discharge capacity of 455 mAh/g was accounted for TiN-900 which is higher than that of TiN-800 and TiN-1000 at 393 and 443 mAh/g respectively (Figure 3c). The discharge capacity of TiN-900 first decreases during the first twenty cycles followed by gradual increase up to fiftieth cycle (486 mAh/g) before another trivial decrease. This initial decrease followed by slow increase after the first twenty cycles were also observed in TiN-800 and TiN-1000. This result is exemplary compared to other previous reports about nanostructured TiN and other metal nitride composites^{36, 37, 49, 50} and the highest capacity reported ever for TiN. Such stability reveals that TiN is a promising anode for LIBs as it is much better than the conventional graphite anodes.

To further verify the superiority of TiN-900 among the electrodes, galvanostatic discharge/charge (lithium insertion/ lithium extraction) measurements were carried out at various increasing current densities. TiN-900 delivers a decent discharge capacity of 460, 385, 332, 288 mAh/g at 335, 670, 1005 and 1675 mA/g respectively (Figure 3d). Upon all the increase in the current densities, TiN-900 displayed continuously higher capacities (288 mAh/g) than that of TiN-800 and TiN-1000 at 189 and 248 mAh/g (at 1625 mA/g) respectively. This indicates that the TiN-900 exhibits higher rate capability among the TiN samples tested.

Electrochemical impedance spectroscopy (EIS) measurement was performed in order to study the conductivity and internal resistance of the TiN samples. EIS study was carried out at a frequency range of 100 kHz to 0.01 Hz. The charge transfer resistance (the diameter of the semicircle in the impedance spectrum) of TiN-900 at the high frequency was fiercely smaller than that of TiN-800 and TiN-1000 showing that the TiN-900 has better conductivity and low charge-transfer resistance than TiN-800 and TiN-100 (Figure 3d). The EIS study also demonstrates the supremacy of TiN-900.

Using the flexible TiN-900 anode and LiCoO_2 cathode, we then built a thin, lightweight, and flexible $\text{LiCoO}_2/\text{TiN-900}$ full battery. The $\text{LiCoO}_2/\text{TiN-900}$ full battery electrodes with surface area of 2 cm^2 were sealed in an Al bag. Figure 4a show the graphical structure of the flexible LIBs. This flexible battery is able to power a red light-emitting diode (LED) when bent as demonstrated in Figure 4b. The initial discharge capacity of the battery is 167 mAh/g at the normal position with capacity retention of 95% after 120 cycles

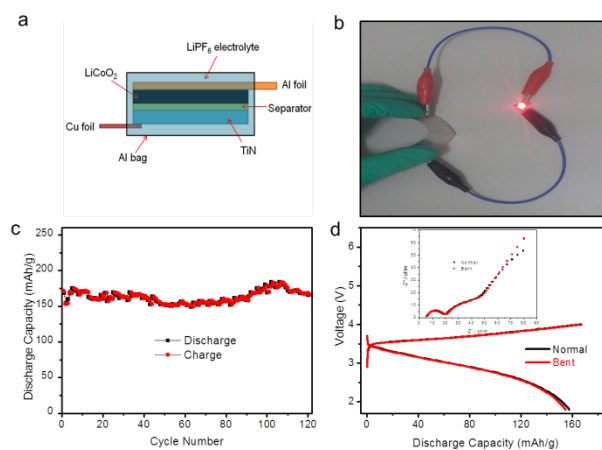


Figure 4. (a) Schematic structure of a flexible Li-ion battery. (b) Demonstration of the $\text{LiCoO}_2/\text{TiN-900}$ full battery powering a red LED at the bending position. (c) Cyclic stability of $\text{LiCoO}_2/\text{TiN-900}$ up to 120 cycles. (d) Charge-discharge curves of $\text{LiCoO}_2/\text{TiN-900}$ at the normal and bent position after the 5th and 10th cycle respectively. Inset: Nyquist plot of $\text{LiCoO}_2/\text{TiN-900}$ at the normal and bent position.

(Figure 4c). To further justify the flexibility of the $\text{LiCoO}_2/\text{TiN-900}$ full battery, the battery was cycled for another 10 cycles as presented in Figure S6. When the battery capacity becomes stable at the 5th cycle (157 mAh/g), the battery was then bent for another five cycles retaining a capacity of 154 mAh/g with a Coulombic efficiency of 98% (Figure S4). The charge/discharge curves plotted for the $\text{LiCoO}_2/\text{TiN-900}$ full battery after the 5th cycle at the normal position and the 10th cycle at that bent position were very similar (Figure 4d). The impedance of the battery at the normal and bent position is almost the same when the Nyquist plot of the battery was plotted after performing the EIS measurements (Figure 4d inset). This result verifies that the bending has no negative effect on the resistance of the battery.

Conclusions

In conclusion, we have synthesized TiN nanowires by hydrothermal method and annealing on a carbon fabric. When utilized in a half-cell, the synthesized TiN nanowires could deliver high reversible capacity of 566 mAh/g. A discharge capacity of 455 mAh/g at 335 mA/g was retained after 100 cycles resulting in capacity retention of 80% and at high current density of 1675 mA/g, the TiN electrode still exhibits discharge capacity of 288 mAh/g. The TiN NW anode was further used as anode in the fabrication of flexible LIBs and this device demonstrated high flexibility and bendability with considerable electrochemical performance. Our results propose that the synthesis of TiN nanowires could be a dependable approach to boost the electrochemical properties of metal nitride anode material and their application in flexible full LIBs.

Acknowledgements

We acknowledge the financial support by the Natural Science Foundations of China (212732909, 91323101 and J1103305), the Natural Science Foundations of Guangdong Province (S2013030013474), the Research Fund for the Doctoral Program of Higher Education of China (20120171110043), and

the Young Teacher Starting-up Research of Sun Yat-Sen University.

Notes and references

^aMOE of the Key Laboratory of Bioinorganic and Synthetic Chemistry, KLGHEI of Environment and Energy Chemistry, School of Chemistry and Chemical Engineering, Sun Yat-Sen University, Guangzhou 510275, People's Republic of China. Email: luxh6@mail.sysu.edu.cn (X. H. Lu); chedhx@mail.sysu.edu.cn (Y. X. Tong) Fax: +86 20 84112245; Tel: +86 20 84110071

^bSchool of Chemistry and Chemical Engineering, Guangdong Pharmaceutical University, Guangzhou 510006, China

Electronic Supplementary Information (ESI) available: [details of any supplementary information available should be included here]. See DOI: 10.1039/c000000x/

- L. Peng, X. Peng, B. Liu, C. Wu, Y. Xie and G. Yu, *Nano Lett.*, 2013, **13**, 2151.
- S.-Y. Lee, K.-H. Choi, W.-S. Choi, Y. H. Kwon, H.-R. Jung, H.-C. Shin and J. Y. Kim, *Energy Environ. Sci.*, 2013, **6**, 2414.
- B. Scrosati and J. Garche, *J. Power Sources*, 2010, **195**, 2419.
- X. Huang, B. Sun, S. Chen and G. Wang, *Chem. An Asian J.*, 2014, **9**, 206.
- X. Lu, M. Yu, G. Wang, T. Zhai, S. Xie, Y. Ling, Y. Tong and Y. Li, *Adv. Mater.*, 2013, **25**, 267.
- M. Yu, Y. Zeng, C. Zhang, X. Lu, C. Zeng, C. Yao, Y. Yang and Y. Tong, *Nanoscale*, 2013, **5**, 10806-10810.
- C. Wu, X. Lu, L. Peng, K. Xu, X. Peng, J. Huang, G. Yu and Y. Xie, *Nat. commun.*, 2013, **4**, 2341.
- N. Li, G. Zhou, F. Li, L. Wen and H. M. Cheng, *Adv. Funct. Mater.*, 2013, **23**, 5429.
- K. Fu, O. Yildiz, H. Bhanushali, Y. Wang, K. Stano, L. Xue, X. Zhang and P. D. Bradford, *Adv. Mater.*, 2013, **25**, 5109-5114.
- S. W. Kim, J. H. Yun, B. Son, Y. G. Lee, K. M. Kim, Y. M. Lee and K. Y. Cho, *Adv. Mater.*, 2014, DOI: 10.1002/adma.201305600.
- P. Zhang, J. Qiu, Z. Zheng, G. Liu, M. Ling, W. Martens, H. Wang, H. Zhao and S. Zhang, *Electrochim. Acta*, 2013, **104**, 41.
- B. Liu, J. Zhang, X. Wang, G. Chen, D. Chen, C. Zhou and G. Shen, *Nano Lett.*, 2012, **12**, 3005.
- H. Yu, C. Zhu, K. Zhang, Y.-J. Chen, C. Li, P. Gao and Q. Ouyang, *J. Mater. Chem. A*, 2014, **2**, 4551.
- Y.-T. Liu, X.-D. Zhu, Z.-Q. Duan and X.-M. Xie, *Chem. Commun.*, 2013, **49**, 10305.
- H. Lin, W. Weng, J. Ren, L. Qiu, Z. Zhang, P. Chen, X. Chen, J. Deng, Y. Wang and H. Peng, *Adv. Mater.*, 2013, **26**, 1217.
- J. Deng, L. Xi, L. Wang, Z. Wang, C. Chung, X. Han and H. Zhou, *J. Power Sources*, 2012, **217**, 491.
- C. Wu, P. Yin, X. Zhu, C. OuYang and Y. Xie, *J. Phys. Chem. B*, 2006, **110**, 17806.
- J. Liu, Y. Li, X. Huang, R. Ding, Y. Hu, J. Jiang and L. Liao, *J. Mater. Chem.*, 2009, **19**, 1859.
- P. Nie, L. Shen, H. Luo, B. Ding, G. Xu, J. Wang and X. Zhang, *J. Mater. Chem. A*, 2014, DOI: 10.1039/C4TA00062E.
- L. Shen, H. Li, E. Uchaker, X. Zhang and G. Cao, *Nano Lett.*, 2012, **12**, 5673.
- T. Graziani and A. Bellosi, *J. Mater. Sci. Lett.*, 1995, **14**, 1078.
- K. Kamiya, T. Nishijima and K. Tanaka, *J. Am. Cer. Soc.*, 1990, **73**, 2750.
- H. Zheng, K. Oka and J. D. Mackenzie, Preparation of Titanium Carbonitride Coatings by the Sol-Gel Process, 1992.
- C. F. Windisch, J. W. Virden, S. H. Elder, J. Liu and M. H. Engelhard, *J. Electrochem. Soc.*, 1998, **145**, 1211.
- M. Ritala, M. Leskelä, E. Rauhala and P. Haussalo, *J. Electrochem. Soc.*, 1995, **142**, 2731.
- C. J. Carmalt, A. H. Cowley, R. D. Culp, R. A. Jones, Y.-M. Sun, B. Fitts, S. Whaley and H. W. Roesky, *Inorg. Chem.*, 1997, **36**, 3108.
- J. Elam, M. Schuisky, J. Ferguson and S. George, *Thin Solid Films*, 2003, **436**, 145.
- B. Avsarala and P. Haldar, *Electrochim. Acta*, 2010, **55**, 9024.
- I. Milošv, H. H. Strehblow, B. Navinšek and M. Metikoš - Huković, *Surf. Interface Anal.*, 1995, **23**, 529.
- X. Lu, G. Wang, T. Zhai, M. Yu, S. Xie, Y. Ling, C. Liang, Y. Tong and Y. Li, *Nano Lett.*, 2012, **12**, 5376.
- Y. Qiu, K. Yan, S. Yang, L. Jin, H. Deng and W. Li, *ACS nano*, 2010, **4**, 6515.
- M. Q. Snyder, S. A. Trebukhova, B. Ravdel, M. C. Wheeler, J. DiCarlo, C. P. Tripp and W. J. DeSisto, *J. Power Sources*, 2007, **165**, 379-385.
- I. s. Kim, P. Kumta and G. Blomgren, *Electrochem. Solid State Lett.*, 2000, **3**, 493.
- M. Liu, X. Li, H. Ming, J. Adkins, X. Zhao, L. Su, Q. Zhou and J. Zheng, *New J. Chem.*, 2013, **37**, 2096.
- Y. Yue, P. Han, X. He, K. Zhang, Z. Liu, C. Zhang, S. Dong, L. Gu and G. Cui, *J. Mater. Chem.*, 2012, **22**, 4938.
- G. Cui, L. Gu, A. Thomas, L. Fu, P. A. van Aken, M. Antonietti and J. Maier, *ChemPhysChem*, 2010, **11**, 3219.
- D. Lei, T. Yang, B. Qu, J. Ma, Q. Li, L. Chen and T. Wang, *Science and Educ.*, 2014, **2**, 1.
- H. Zheng, T. Zhai, M. Yu, S. Xie, C. Liang, W. Zhao, S. C. I. Wang, Z. Zhang and X. Lu, *J. Mater. Chem. C*, 2013, **1**, 225.
- J. H. Bang and K. S. Suslick, *Adv. Mater.*, 2009, **21**, 3186.
- X. Lu, T. Liu, T. Zhai, G. Wang, M. Yu, S. Xie, Y. Ling, C. Liang, Y. Tong and Y. Li, *Adv. Energy Mater.*, 2013, DOI: 10.1002/aenm.201300994.
- S. Dong, X. Chen, L. Gu, X. Zhou, H. Xu, H. Wang, Z. Liu, P. Han, J. Yao and L. Wang, *ACS Appl. Mater. Interfaces*, 2010, **3**, 93.
- M. Stoehr, C.-S. Shin, I. Petrov and J. Greene, *J. Appl. Phys.*, 2011, **110**, 083503.
- M. O. Thotiyl, T. R. Kumar and S. Sampath, *J. Phys. Chem. C*, 2010, **114**, 17934.

Journal Name

44. M.-H. Chan and F.-H. Lu, *Thin Solid Films*, 2009, **517**, 5006.
45. N. Pereira, L. Klein and G. Amatucci, *J. Electrochem. Soc.*, 2002, **149**, A262.
46. Z.-W. Fu, Y. Wang, X.-L. Yue, S.-L. Zhao and Q.-Z. Qin, *J. Phys. Chem. B*, 2004, **108**, 2236.
47. H. Han, T. Song, J.-Y. Bae, L. F. Nazar, H. Kim and U. Paik, *Energy Environ. Sci.*, 2011, **4**, 4532.
48. J.-Y. Liao, D. Higgins, G. Lui, V. Chabot, X. Xiao and Z. Chen, *Nano Lett.*, 2013, **13**, 5467.
49. F. Gillot, J. Oró-Solé and M. R. Palacín, *J. Mater. Chem.*, 2011, **21**, 9997.
50. K. Zhang, H. Wang, X. He, Z. Liu, L. Wang, L. Gu, H. Xu, P. Han, S. Dong and C. Zhang, *J. Mater. Chem.*, 2011, **21**, 11916.

Graphical Abstract

